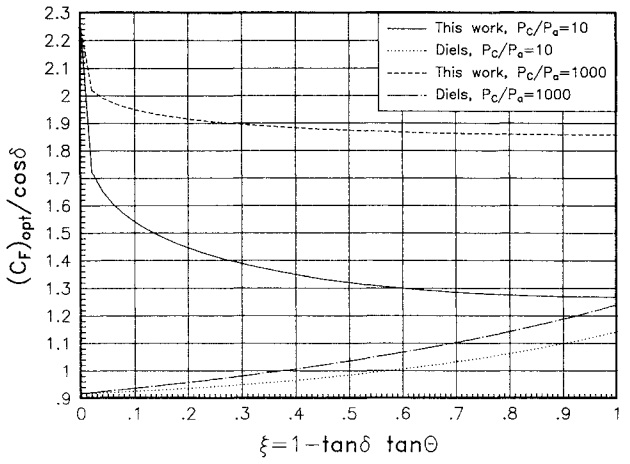

Fig. 3 Optimum performance comparison.

$p_e/p_a = 0$. For this case, there is no optimum (only an asymptotically approached maximum value), and Eq. (6) shows that missile axial thrust is independent of atmospheric pressure. These results agree with the numerical calculations of Lilley and Hoffman.[2] For all other cases, the optimum exit pressure will be less than the atmospheric pressure.

Figure 2 presents results of calculations of the optimal p_e/p_a for a range of chamber pressure and specific heat ratios. The results show weak sensitivity to each of these parameters.

Figure 3 illustrates the variation of a normalized thrust coefficient given by

$$C_F/\cos\delta = F_v/(p_c A_t \cos\delta) \tag{17}$$

as a function of ξ for pressure ratios of 10 and 1000 and $\gamma = 1.2$. The results clearly show that Diels' solution does not maximize the thrust along the missile axis.

Conclusions

The solution for maximum thrust along the missile's axis, found by Diels, maximizes thrust per unit exit area rather than the thrust magnitude. The solution for maximum missile axial thrust has been found for one-dimensional flow in which exit Mach lines are not swallowed. The solution shows that the optimum exit pressure is less than or equal to the atmospheric pressure for a canted, scarfed nozzle. When the exit plane of the canted, scarfed nozzle is parallel to the missile's axis, thrust is independent of atmospheric pressure, and no optimum condition exists.

Acknowledgment

This work was supported by the Ballistic Missile Defense Advanced Technology Center; Program Manager, R. Reviera. Support was also provided by the Propulsion Directorate of the U.S. Army Missile Command.

References

[1]Phillips, W. W., "Thrust Coefficients, Thrust Deflection Angles, and Non-Dimensional Moments for Nozzles with Oblique Exits," Boeing Co., Seattle, WA, Rept. D2-125619-1, March 1968.

[2]Lilley, J. S. and Hoffman, J. D., "Performance Analysis of Scarfed Nozzles," *Journal of Spacecraft and Rockets*, Vol. 23, Jan.-Feb. 1986, pp. 55-62.

[3]Diels, M. F., "Forces on Nozzles with Skewed Exits," Aerojet-General Corp., Sacramento, CA, TM 4510:59-10, Jan. 1958.

[4]Hoffman, J. D. and Zucrow, M. J., *Gas Dynamics*, Vol. 1, Wiley, New York, 1976, p. 235.

Comparing Hydrogen and Hydrocarbon Booster Fuels

James A. Martin*
NASA Langley Research Center
Hampton, Virginia

Introduction

HYDROGEN and hydrocarbon fuels have been compared for use in rocket vehicles in the past. The purpose of this Note is to show more clearly how the differences in the fuels produce differences in vehicles.

Vehicle

The vehicle considered is illustrated in Fig. 1. It could represent an expendable first stage or, with some adjustments, a reusable vehicle. The gross mass m_0 is related to the dry mass m_d by the ideal rocket equation

$$m_0 = m_d e^{v/u}$$

where v is the velocity increment and u the effective exhaust velocity.

The dry mass is the sum of the fixed mass m_f, the tank mass m_t, and the engine mass m_e,

$$m_d = m_f + m_t + m_e$$

The fixed mass represents the payload, upper stages, and other masses that do not change as the propulsion requirements change. The tank mass is a function of the propellant mass $(m_0 - m_d)$

$$m_t = T(m_0 - m_d)$$

where T is a constant for each fuel. The engine mass is a function of the gross mass

$$m_e = Em_0$$

where E is also a constant for each fuel.

These equations can be solved algebraically to give

$$\frac{m_d}{m_f} = \frac{1}{1 + T - (E+T)e^{v/u}}$$

and

$$\frac{m_0}{m_f} = \frac{m_d}{m_f} e^{v/u}$$

Results

The Appendix provides the basis for the selection of the values of the constants given in Table 1. With these constant values, m_0/m_f is shown as a function of velocity in Fig. 2. Figure 3 shows the equivalent results for m_d/m_f.

The gross mass increases with velocity more rapidly with hydrocarbon fuel than with hydrogen fuel. This is expected because of the difference in effective exhaust velocity. While

Received Aug. 7, 1986.

*Aerospace Engineer, Space Systems Division. Associate Fellow AIAA.

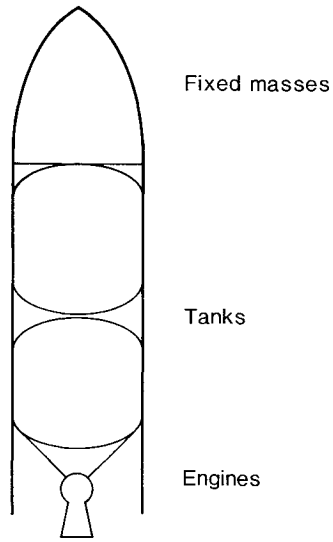

Fig. 1 Booster elements.

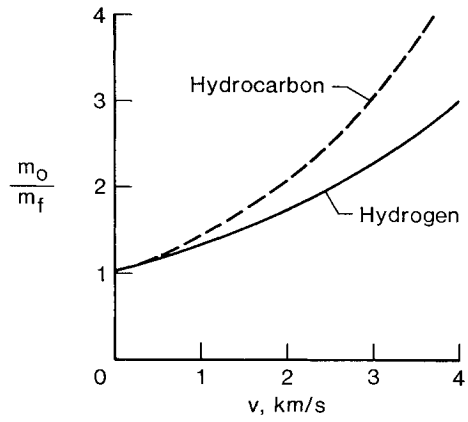

Fig. 2 Effect of fuel on gross mass.

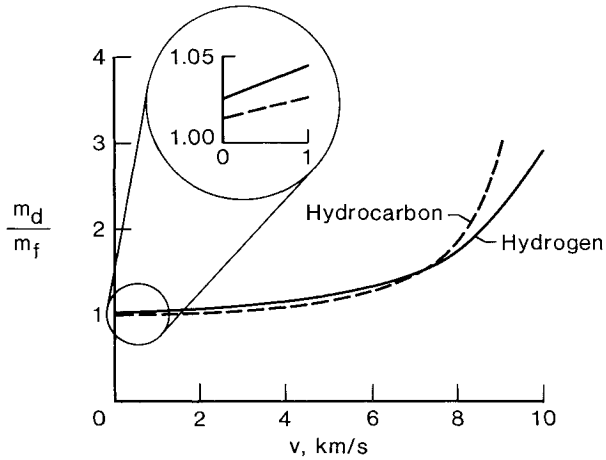

Fig. 3 Effect of fuel on dry mass.

Table 1 Typical constant values

Fuel	Hydrogen	Hydrocarbon
E	0.024	0.014
T	0.046	0.016
u, m/s	4175	2891

gross mass is useful in understanding the differences between vehicles, the dry mass is a much better indicator of vehicle costs.

At velocity requirements greater than 8 km/s, the dry mass results (Fig. 3) are similar to the gross mass results. That is, the hydrocarbon curve increases more rapidly than the hydrogen curve. This is also expected because of the difference in effective exhaust velocity. On the other hand, at lower velocity requirements, the hydrocarbon curve is below the hydrogen curve. To understand this result, it is important to understand the relationship of the curves at low-velocity requirements, shown in the inset.

The intercept of the curves is given by the dry mass equation at $v=0$,

$$\left(\frac{m_d}{m_f}\right)_{v=0}=\frac{1}{1-E}$$

The intercept values are 1.025 for hydrogen and 1.014 for hydrocarbon. Physically, in the $v=0$ case, the vehicle can be thought of as having enough engines to lift the fixed mass and no propellant. Because hydrocarbon engines have less mass for a given thrust requirement, E and the intercept are less.

The slope of each curve near the intercept can be found by differentiating the dry mass equation and evaluating the result at $v=0$. The result is

$$\left[\frac{\mathrm{d}(m_d/m_f)}{\mathrm{d}v}\right]_{v=0}=\frac{E+T}{u(1-E)^2}$$

The slopes are 0.018 km^{-1}/s for hydrogen and 0.011 km^{-1}/s for hydrocarbon. Physically, this results because the energy needed for a 1 km/s velocity increment can be stored in a smaller tank with hydrocarbon fuel than with hydrogen fuel. Another measure is the impulse density, which is greater for hydrocarbon fuel. Also, the mass of the engines needed to lift the propellant required for a 1 km/s velocity increment is less with hydrocarbon fuel because E/u is less.

Given that both the intercept and the slope are less with hydrocarbon fuel, it is obvious that hydrocarbon fuel will be preferred for low-velocity requirements. As v increases, the hydrocarbon curve turns upward and the curves cross. The value of v at which the curves cross may vary widely with different constant values, but the existence of a crossing is fairly certain.

Dual-Fuel Vehicles

Vehicles with both hydrogen and hydrocarbon fuels attempt to take advantage of the low intercept and slope of hydrocarbon fuel at low velocity and to take advantage of the slope of the hydrogen curves at higher velocities. These vehicles have been discussed in numerous publications in the literature.

Conclusion

This comparison of hydrogen and hydrocarbon fuels for rocket vehicles has shown how hydrocarbon fuel leads to lower vehicle dry mass for low-velocity requirements. For higher-velocity requirements, hydrogen fuel provides lower dry mass.

Appendix

The J-2 and H-1 engines provide an appropriate comparison between engines with hydrogen or hydrocarbon fuel. The historical English units will be used only to get the dimensionless constants. Each delivers a vacuum thrust of about 230,000 lb (1023 kN), has a gas generator cycle, and was built for the Apollo program. The dry mass of the J-2 is 3576 lb (1622 kg) and of the H-1 2030 lb (921 kg). Assuming the vehicle thrust-to-weight ratio is 1.3 and adding 20% to account for sea-level thrust loss and thrust structure, the engine constant for hydrogen fuel is

$$E = (3676/230{,}000)(1.3)(1.2)$$

$$= 0.024$$

The equivalent value for hydrocarbon fuel is

$$E = (2030/230{,}000)(1.3)(1.2)$$

$$= 0.014$$

The specific impulse of the J-2 is 426 s and the effective exhaust velocity is the specific impulse multiplied by the reference acceleration of gravity, 9.8 m/s^{-2}, which gives 4175 m/s. For the H-1, the specific impulse is 295 s and the effective exhaust velocity is 2891 m/s.

The characteristics of the Space Shuttle external tank, before some of the mass-reduction programs, were used to evaluate T. The total dry mass was 75,834 lb (34.4 Mg). The hydrogen tank mass was 31,670 (14.4 Mg) and the hydrogen tank volume was 53,515 ft^3 (1515 m^3). The tank mass per unit volume k is given by

$$k = 31{,}670/53{,}515$$

$$= 0.59 \text{ lb/ft}^3 \ (9.5 \text{ kg/m}^3)$$

The corresponding calculation for the oxygen tank is

$$k = 12{,}663/19{,}609$$

$$= 0.65 \text{ lb/ft}^3 \ (10.3 \text{ kg/m}^3)$$

These values indicate that k is a weak function of the density of the propellant. To get the total external tank mass, the mass of the individual tanks must be multiplied by

$$\frac{72{,}000}{31{,}670 + 12{,}662} = 1.62$$

where the total mass is reduced somewhat for systems on the external tank that are not appropriate for this analysis.

The bulk density of oxygen and hydrogen at 6:1 mixture ratio is 22 lb/ft^3 (350 kg/m^3). This is between oxygen and hydrogen and a k value of 0.62 is selected. The tank constant is calculated

$$T = (0.62/22)1.62$$

$$= 0.046$$

For hydrocarbon fuel, the bulk density is 64 lb/ft^3 (1030 kg/m^3). The k value selected is 0.65 and the tank constant is calculated as

$$T = (0.65/64)1.62$$

$$= 0.016$$

Electron Collection by Multiple Objects within a Single Sheath

V. A. Davis,* M. J. Mandell,* and I. Katz†
S-CUBED Division, Maxwell Laboratories
La Jolla, California

Introduction

In order to design reliable high-power spacecraft, it is necessary to understand the interactions between high-voltage power systems and the space plasma. A few space flight experiments with exposed high-voltage conductors have been flown[1,2] and more are being planned. NASCAP/LEO, a computer program that simulates in three dimensions the interaction of high-voltage surfaces with plasma, has been developed to extend the limited experimental data and aid in system design. NASCAP/LEO solves Poisson's equation and computes currents by following representative particle trajectories.[3] Although this model has been compared with the gross current through a sheath,[4] previously there has been no experimental data on how the currents are distributed among different high-voltage objects within the same plasma sheath. In this Note we report calculations that are directly comparable with recent ground test data published by Carruth[5] designed specifically to measure current distribution within a sheath. The conclusion is that, for at least this limited set of data, the electron charge transport within the sheath is dominated by quasistatic space charge fields, and that if anomalous transport between conductors exists, it is not of sufficient magnitude to influence the current measurements.

Carruth's Experiment

Carruth's experimental setup[5] consisted of a test article and two emissive probes in a tank along with a hollow cathode plasma source. The test article was a circuit board covered with a 2-mil Kapton sheet except for two slits under which were exposed conducting electrodes. The configuration modeled in the present paper has a slit width of 0.64 cm and a slit spacing of 3 cm. The emissive probes were suspended above the center of the circuit board, at distances of 0.8 cm and 1.8 cm, and could be moved normal to the slit direction. Current was collected only from the center 4.2-cm section of each of the slits in order to avoid fringing effects. The plasma source created an argon plasma with a temperature of 2–3 eV and a plasma density of $2\text{–}4 \times 10^6/\text{cm}^3$.

NASCAP/LEO Calculation

Carruth's experiment was simulated using the NASA Charge Analyzer Program for Low Earth Orbit (NASCAP/LEO)[3] code, a computer code designed to study the interaction between a high-voltage spacecraft and a short Debye length plasma. In particular, NASCAP/LEO predicts the plasma currents and the electrostatic potentials both on insulating surfaces and in the surrounding plasma. The kernel of NASCAP/LEO is an electrostatic potential solver that uses analytical formulas for space charge and either potential or electric field boundary conditions at each surface cell. The only code input variables are the ambient plasma parameters and a description of the test object.

The printed circuit board was modeled as a rectangular solid with a top surface of Kapton with silver strips. The slits were biased with respect to plasma ground. The code automatically

Received May 7, 1987; revision June 15, 1987.

*Staff Scientist. Member AIAA.
†Program Manager. Member AIAA.